CCS Chemistry

IMMEDIATE ONLINE ACCEPTED (IOA) ARTICLE

This article presented here has been peer reviewed and accepted for publication in *CCS Chemistry*. The present version of this manuscript has been posted at the request of the author prior to copyediting and composition and will be replaced by the final published version once it is completed. The DOI will remain unchanged.

IOA Posting Date: December 29, 2022

TITLE: Implanting Built-in Electric Field in Hetero-metallic Phthalocyanine Covalent Organic Frameworks for Light-assisted CO_2 Electroreduction

AUTHORS: Xi Tian, Xin Huang, Jing-Wen Shi, Jie Zhou, Can Guo, Rui Wang, Yi-Rong Wang, Meng Lu, Qi Li, Yifa Chen, Shun-Li Li & Ya-Qian Lan

DOI: 10.31635/ccschem.022.202202519

CITE THIS: *CCS Chem.* **2022**, Just Accepted. DOI: 10.31635/ccschem.022.202202519

RESEARCH ARTICLE

Implanting Built-in Electric Field in Hetero-metallic Phthalocyanine Covalent Organic Frameworks for Light-assisted CO_2 Electroreduction

Xi Tian[1†], Xin Huang [1†], Jing-Wen Shi [1†], Jie Zhou [2], Can Guo [2], Rui Wang [1], Yi-Rong Wang [2], Meng Lu [2], Qi Li[1], Yifa Chen[2]*, Shun-Li Li[2] & Ya-Qian Lan [2]*

[1]*School of Chemistry and Materials Science, Nanjing Normal University, Nanjing 210023.*

[2]*School of Chemistry, South China Normal University, Guangzhou, 510006.*

Homepage : http://www.yqlangroup.com/

**Corresponding authors Y. C. E-mail: chyf927821@163.com; Y-Q. L. E-mail: yqlan@njnu.edu.cn*

[†] *Xi Tian, Xin Huang and Jing-Wen Shi contributed equally to this work*

Abstract

Strategy that enables introducing bimetallic active sites is desired for the exploration of light-sensitive covalent-organic-frameworks (COFs) based electrocatalysts in light-assisted CO_2-electroreduction. Herein, salphen-pockets have been implanted into phthalocyanine-based COFs through the elaborate design of structure-struts and thus-produced NiPc-DFP-M COF (M = Ni and Co) possess the advantages of controllably bimetallic centers with different coordination-environments, outstanding light-sensitivity, and built-in electric-field effect that can be successfully applied in light-assisted CO_2 electroreduction. Notably, the optimally hetero-metallic NiPc-DFP-Co COF presents a high FE_{CO} (~100%) in a wide potential-range of -0.7 V to -1.1 V and ~70% energy-efficiency (-0.7 V) under light-irradiation, which is superior to mono-/homo-metallic COFs and under dark conditions. The high performance can be ascribed to the synergistic effect of NiPc and Co-salphen pockets that can largely reduce the rate-determining energy-barrier and enhance the electron-density to boost the light-assisted activity as supported by DFT-calculations.

Keywords: **Built-in Electric Field, Hetero-metallic Phthalocyanine, Light-assisted, CO_2 Electroreduction**

Introduction

Nowadays, the problems of rising sea level and global warming caused by the excessive CO_2 emission is becoming more and more serious, and much attention have been paid around the world to potentially address the challenging issue with diverse newly developed techniques.[1, 2] Among them, electrocatalytic carbon dioxide reduction reaction (CO_2RR) has been widely studied and regarded as one of the efficient ways to convert CO_2 into high value-added chemicals (e.g., CO, CH_4, C_2H_4, formic acid, methanol or ethanol, etc.).[3-5] Nevertheless, owing to the inherent thermodynamic and kinetic sluggishness of electrocatalytic CO_2RR and competitive kinetically-favored H_2 generation reaction, electrocatalytic CO_2RR generally faces disadvantages like low selectivity or energy efficiency.[6-9] Exploring efficient electrocatalytic CO_2RR electrocatalysts with suitable advanced assisted techniques is one of the promising approaches to improve the efficiency of electrocatalytic CO_2RR. Besides, there might exist property barriers by relying on electrocatalysts with single active site or simple functionality, thus introducing other assisted functional sites as auxiliary units is of great significance for electrocatalytic CO_2RR conquer its inherent barriers. Directional structure designing of catalysts, regulating the catalytic environments, and modulating the active sites or functional groups might be potential strategies to reduce the overpotential of electrocatalytic CO_2RR, promote the electron transfer and expose active sites, which are beneficial to improve the efficiency of electrocatalytic CO_2RR.[10-12] Besides, it is relatively limited by the electricity energy itself to improve the efficiency of electrocatalytic CO_2RR and other techniques like light-assisted ones are favorable for improving the catalytic activity of electrocatalytic CO_2RR.[13, 14] Therefore, designing and introducing functional sites to form bi-/multi-functional active sites that enable the applications in light-assisted electrocatalysis are highly desirable yet still unmet.

As a kind of heterogeneous catalyst, covalent organic frameworks (COFs) have the advantages of well-defined structures and strong design controllability, porosity, large specific surface area and high stability, etc.[15, 16] So far, COFs (e.g., COF-366-Co[17] , COF-300-AR[18] and COF-366-Cu[14] , etc.) have been studied in electrocatalytic CO_2RR. For their potential applications as the light-assisted electrocatalytic CO_2RR electrocatalysts, COFs need to meet the high

This article presented here has been accepted for publication in CCS Chemistry and is posted at the request of the author prior to copyediting and composition.
© 2022 Chinese Chemical Society.

RESEARCH ARTICLE

requirements of catalytic active sites, light-absorbing structural units, electron-hole separation and migration capability, and adequate stability.[19] In COFs, the commonly used electrocatalytic units with light-absorbing ability are porphyrin or phthalocyanine (Pc) based functional groups.[20, 21] In particular, phthalocyanine, an 18π aromatic macrocyclic compound with M-N_4 (M = Co, Ni, Cu, and Fe, etc.) CO_2RR active sites, is a typical light-sensitive structural unit.[22, 23] Its electronic property will change greatly under light driving, so it has been widely studied in photocatalysis or electrocatalysis, and even photo-electric coupling reactions.[24-26] So far, Pc-based COFs have been designed and synthesized for electrocatalytic CO_2RR owing to their large conjugated and conductive structures that are favorable for the electron transfer to the active sites.[27, 28] However, the application of Pc-based COFs in electrocatalytic CO_2RR is still limited for the following reasons: 1) most of reported Pc-based COFs only possess single active site, and the introduction of functional sites or designed bimetallic active sites for synergistic catalysis have been rarely reported;[29, 30] 2) the syntheses of crystalline bi-/multi-functional Pc-based COFs with built-in electric field effect remain a challenge and some of them can only result in Pc-based polymers with unclear structures, which is hard to investigate the specific structure-property relationship or mechanism in electrocatalytic CO_2RR without a clear crystallographic model;[31-33] 3) other assistance techniques like light-assisted ones that can be integrated in the system to improve the efficiency of electrocatalytic CO_2RR are still rare.[19] Therefore, the investigation of electrocatalytic CO_2RR based on bi-/multi-functional Pc-based COFs under the assistance of light holds much potential to address the potential issues as mentioned above, yet such powerful systems are still hard to achieve no matter in electrocatalyst design or technique implementation.

Herein, a series of bimetallic Pc-based NiPc-DFP-M COF (M = Ni and Co) are produced through the assembly of 2,3,9,10,16,17,23,24-octaamino-phthalocyaninato nickel II (NiPc-8NH_2) and 2,6-diformylphenyl (DFP) (Figure 1a). The synergistic combination of NiPc and metal ions coordinated salphen pockets (M-N_2O_2) can endow these materials with the advantages of CO_2 adsorption/activation, built-in electric field effect and outstanding light-sensitivity, which present superior light-assisted electrocatalytic CO_2RR performances. Notably, best of them, NiPc-DFP-Co COF presents a superior FE_{CO} (~100%) in a wide potential-range of -0.7 V to -1.1 V vs. RHE and a ~70% energy efficiency (-0.7 V)[11] under light-irradiation, which is superior to those of mono-/homo-metallic COFs and under dark conditions. This achieved property is represented to be one of the best performances in reported COFs. Furthermore, the electrocatalytic CO_2RR mechanism of NiPc-DFP-M COF (M = Ni and Co) with diverse metal centers implies that NiPc-DFP-Co COF exhibits the largely decreased energy barrier of the rate determine step owing to the implantation of Co-coordinated salphen pockets (Co-N_2O_2) in electrocatalytic CO_2RR compared with NiPc-DFP-Ni COF and NiPc-DFP COF as revealed by the electrocatalytic performances and the density functional theory (DFT) calculations. This work not only proposes a synergistic catalysis of bimetallic electrocatalysts for light-assisted electrocatalytic CO_2RR, but also provides intuitive understandings of product generation and catalyst optimization for electrocatalytic CO_2RR and beyond.

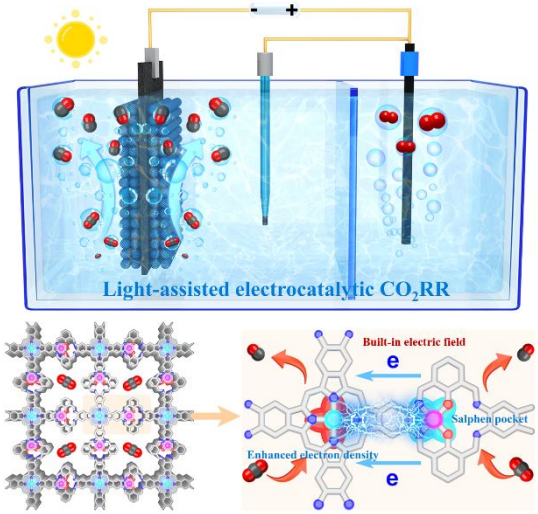

Scheme 1 | *Schematic illustration of the advantages of salphen pocket implanted heteto-metallic Pc-based COFs in light-assisted electrocatalytic CO_2RR.*

Experimental Methods

Synthesis of NiPc-DFP COF

NiPc-8NH_2 (35 mg, 0.05 mmol), 2,6-diformylphenol (DFP) (20 mg, 0.13 mmol), mesitylene (1.5 mL), 1,4-dioxane (0.5 mL) and triethylamine (0.25 mL) were mixed in a Pyrex tube (o.d × length, 19 × 65 mm). After sonication for about 30 min, the tube was flash frozen at 77 K (liquid N_2 bath) and degassed to achieve an internal pressure of ~100 mTorr. After recovering to room temperature, the mixture was heated at 80 ºC and left undisturbed for 72 h. A dark green precipitate was isolated by filtration in buchner funnel through a filter paper with an aperture of 0.25 μm and was washed with MeOH, DMF, CH_2Cl_2, and THF until the filtrate was colorless. The wet sample was transferred to a Soxhlet extractor and washed with THF (48 h). Finally, the product was evacuated at 80 ºC under dynamic vacuum overnight to yield activated sample (40.5 mg).

Syntheses of NiPc-DFP-M COF (M = Ni and Co)

For the preparation of NiPc-DFP-Co COF, NiPc-DFP COF (50.0 mg) and $Co(Ac)_2$ (25.0 mg) were firstly added into 20 mL MeOH. After stirring for 24 h, the suspension was extracted and washed with plenty of methanol and water to remove the excess metal salts. Finally, the product was evacuated at 80 ℃ under dynamic vacuum overnight to obtain dark green solid. Under the same conditions of NiPc-DFP-Co COF, NiPc-DFP-Ni COF was obtained as dark green solid except that $Co(Ac)_2$ was replaced with $Ni(Ac)_2$.

Synthesis of CoPc-DFP COF

The synthesis of CoPc-DFP COF was carried out following the same protocol as that of NiPc-DFP COF except that the

This article presented here has been accepted for publication in CCS Chemistry and is posted at the request of the author prior to copyediting and composition.
© 2022 Chinese Chemical Society.

RESEARCH ARTICLE

$NiPc\text{-}8NH_2$ was replaced with $CoPc\text{-}8NH_2$ (32.0 mg, 0.05 mmol).

Syntheses of CoPc-DFP-M COF (M = Ni and Co)

For the preparation of CoPc-DFP-Co COF, CoPc-DFP COF (50.0 mg) and $Co(Ac)_2$ (25.0 mg) were firstly added into 20 mL MeOH. After stirring for 24 h, the suspension was extracted and washed with plenty of methanol and water to remove the excess metal salts. Finally, the product was evacuated at 80 ℃ under dynamic vacuum overnight to obtain dark green solid. Under the same conditions of CoPc-DFP-Co COF, CoPc-DFP-Ni COF was obtained as dark green solid except that $Co(Ac)_2$ was replaced with $Ni(Ac)_2$.

Results and Discussion

Synthesis and Characterization of NiPc-DFP-M COF (M = Co and Ni

To prepare NiPc-DFP-Ni COF and NiPc-DFP-Co COF, NiPc-DFP COF is firstly prepared through a Schiff base condensation of $NiPc\text{-}NH_2$ and 2,6-diformylphenol (DFP) (Figure 1a, detail see Synthesis Methods). Then, NiPc-DFP-Ni COF and NiPc-DFP-Co COF are synthesized by the modification of relative metal acetate salts for further characterizations. The detailed COF crystal structure model is simulated using the Materials Studio software package and its unit cell parameters are optimized based on the forcite module. Taking NiPc-DFP-Co COF as an example, the powder X-ray diffraction (PXRD) pattern obtained from the simulation matches well with the experimental results (Rwp = 3.43% and Rp = 2.72%) (Figure 1b), indicating that it has good crystallinity. PXRD pattern and simulation results show an AA packing model with Amm2 space group (Figure 1c), and its unit cell parameters are a = 3.4804 Å, b = c = 29.4331 Å, α = β = γ = 90°. Besides, NiPc-DFP-Co COF exhibits diffraction peaks at 4.39° and 8.74°, which are assigned to the (011) and (031) planes, respectively. The simulated crystal structure shows the layer distance of NiPc-DFP-Co COF is 3.48 Å. Moreover, NiPc-DFP COF and NiPc-DFP-Ni COF are also prepared with high crystallinity as supported by the PXRD patterns (Figure S1 and S2).

In addition, Fourier transform infrared spectroscopy (FT-IR) is performed to further demonstrate the successful syntheses of NiPc-DFP COF and NiPc-DFP-M COF (M = Ni and Co). In FT-IR spectra, the C=O stretching band of DFP at 1683 cm^{-1} and the N-H stretching band of $NiPc\text{-}8NH_2$ monomer at 3199-3350 cm^{-1} disappear along with a peak belonging to the C=N stretching vibration band appears at 1619 cm^{-1} for all of them, indicating the successful formation of C=N bond (Figure S3 and S4).[34, 35] Besides, a new neighboring peak around 1600 cm^{-1}, belonging to the C=N groups with metal coordination in salphen pockets, is observed, which indicates the successful syntheses of NiPc-DFP-Co COF and NiPc-DFP-Ni COF (Figure S3 and S4).[36] In addition, the X-ray photoelectron spectroscopy (XPS) test has performed to prove the syntheses of COFs. The XPS spectral analysis of the NiPc-DFP COF shows that the high-resolution N 1s spectrum fits into two components including C-N=C (398.6 eV) and C=N-Ni (400.6 eV), confirming the existence of M-N bond in this structure (Figure S5).[35] In the Ni 2p XPS spectrum, the binding energies of Ni $2p_{3/2}$ and Ni $2p_{1/2}$ are 855.6 and 873.0 eV, respectively, which are consistent with Ni (II) states for NiPc-DFP COF and NiPc-DFP-M COF (M = Ni and Co) (Figure S5-7).[31, 37] Besides, the Co 2p XPS spectrum of NiPc-DFP-Co COF shows that Co is successfully coordinated with the salphen pockets, illustrating the +2 oxidation states of Co (Figure S6).[38] Compared with NiPc-DFP COF, the O 1s XPS spectra of NiPc-DFP-Ni COF and NiPc-DFP-Co COF are fitted into two components, which belong to C-O and M-O, respectively (Figure S6 and S7).[39] Inductively coupled plasma optical emission spectrometer (ICP-OES) shows that the specific contents of Ni and Co are calculated to be ~4.33% and ~5.50% in NiPc-DFP-Co COF, respectively (Table S1).

The stability of COFs is an important parameter to evaluate their durability property in catalysis. To test it, the samples are soaked in different solvents (i.e. acetone, N, N-dimethylformamide (DMF), tetrahydrofuran (THF), dichloromethane (DCM), methanol (MeOH), HCl (4 M) and NaOH (4 M) at room temperature for at least 1 month (Figure S8). After tests, the NiPc-DFP-Co COF can retain its pristine crystalline structure as revealed by the unchanged positions and intensities of the relative PXRD patterns, indicating the high chemical stability of NiPc-DFP-Co COF. The high stability would provide solid basis for the applications of these COFs in electrocatalytic CO_2RR.

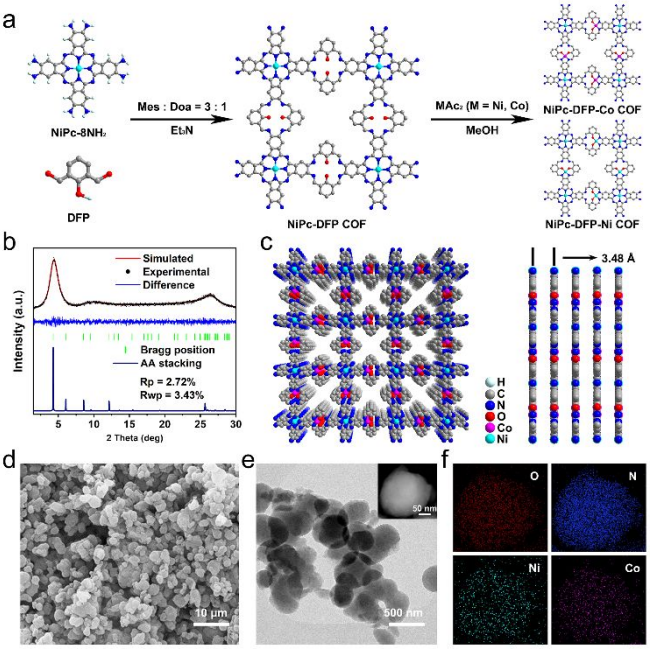

Figure 1 | *Structure and characterization of NiPc-DFP-M COF (M = Co and Ni). **(a)** The syntheses and structures of NiPc-DFP-M COF (M = Co and Ni). **(b)** PXRD patterns of NiPc-DFP-Co COF. **(c)** Top and side view of the AA stacking mode for NiPc-DFP-Co COF. **(d)** SEM image. **(e)** TEM image (insert is the HAADF image). f) EDS elemental mapping images.*

To evaluate the morphology of these samples, scanning electron microscopy (SEM) and transmission electron microscopy (TEM) tests have been performed. The obtained sample displays sphere morphology with a diameter of ~260 nm as proved by the SEM and TEM tests (Figure 1d, e). Energy dispersive X-ray spectroscopy (EDS) mapping

This article presented here has been accepted for publication in CCS Chemistry and is posted at the request of the author prior to copyediting and composition.
© 2022 Chinese Chemical Society.

RESEARCH ARTICLE

images (Figure 1f) show that N, O, Ni and Co elements are uniformly distributed throughout the sphere morphology, indicating that Ni (II) and Co (II) are highly dispersed in NiPc-DFP-Co COF, and also prove that Co (II) is successfully coordinated. In comparison, NiPc-DFP COF and NiPc-DFP-Ni COF also present similar sphere morphology as proved by SEM, TEM and EDS mapping images (Figure S9 and S10). Besides, the CO_2 adsorption tests at 273 K and 298 K show that the prepared NiPc-DFP-Co COF (273 K, 25.2 $cm^3\ g^{-1}$; 298 K, 18.1 $cm^3\ g^{-1}$) exhibits slightly higher adsorption capacity than those of NiPc-DFP COF (273 K, 20.9 $cm^3\ g^{-1}$; 298 K, 13.8 $cm^3\ g^{-1}$) and NiPc-DFP-Ni COF (273 K, 20.9 $cm^3\ g^{-1}$; 298 K, 13.8 $cm^3\ g^{-1}$) (Figure S11).

The electrocatalytic performances of NiPc-DFP-M COF (M = Ni and Co)

The electrocatalytic CO_2RR activity of MPc-DFP-M COF (M = Co and Ni) is investigated using a standard two-compartment H-type cell (separated by Nafion®212) in a $KHCO_3$ aqueous solution (0.5 M, pH = 7.2) saturated with CO_2 as the electrolyte in dark environment. The electrocatalytic performance is evaluated using the current density (j) and the FE of the reduction product as indicators. In these experiments, all potentials are based on reversible hydrogen electrode (RHE) unless otherwise specified. In these Pc-based COFs with modifiable salphen pockets, there are two kinds of metal sites that might affect the possible electrocatalytic CO_2RR properties. To investigate them, CoPc-DFP COF has also been prepared as the contrast sample and modified with Co (CoPc-DFP-Co COF) or Ni (CoPc-DFP-Ni COF) ions for further tests (Figure S12-14). For NiPc-DFP COF, its highest FE_{CO} can be as high as 99.19% at -1.1 V, which is much higher than that of CoPc-DFP COF (61.31%, -0.8 V), CoPc-DFP-Co COF (74.69%, -0.9 V) and CoPc-DFP-Ni COF (62.81%, -0.8 V) (Figure 2b and S15). Therefore, we choose NiPc-DFP COF as the desired platform to modify its salphen pockets with Co and Ni ions to produce relative NiPc-DFP-Co COF and NiPc-DFP-Ni COF, respectively, so as to study the effect of metal-salphen pockets on electrocatalytic CO_2RR. In LSV curves, the NiPc-DFP-Co COF exhibits higher current density and lower onset potential under CO_2 atmosphere than that of Ar atmosphere, indicating the possibility of higher electrocatalytic CO_2RR reaction activity of NiPc-DFP-Co COF (Figure S16). Similar phenomenon has also been detected for NiPc-DFP COF and NiPc-DFP-Ni COF (Figure S17 and S18). Besides, the LSV curves show that the j_{total} of NiPc-DFP-Co COF is much higher than NiPc-DFP-Ni COF and NiPc-DFP COF at different potentials, implying the higher activity of NiPc-DFP-Co COF (Figure 2a).

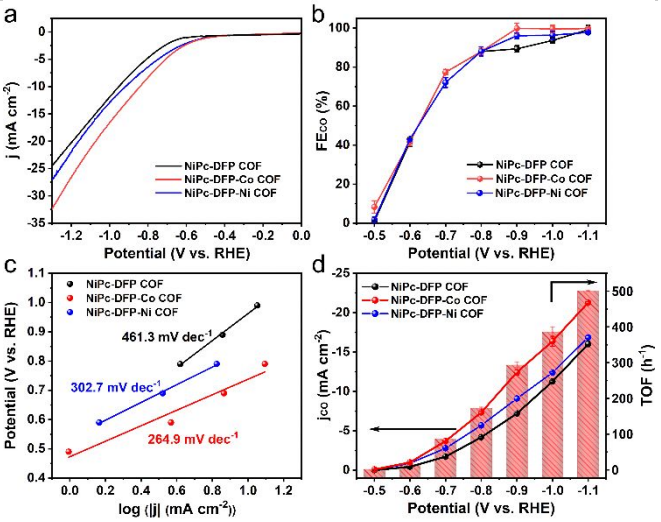

Figure 2 | *Electrocatalytic CO_2RR performances of NiPc-DFP COF, NiPc-DFP-Co COF and NiPc-DFP-Ni COF.* ***(a)*** *LSV curves.* ***(b)*** *Calculated FE_{CO} at the potential range from -0.5 to -1.1 V.* ***(c)*** *Tafel plots.* ***(d)*** *Partial CO current density (j_{CO}) and TOF (h^{-1}).*

In addition to the current density, the electrocatalytic CO_2RR selectivity of samples have also been investigated. For all of them, the detected products are CO and H_2 at a wide potential range of -0.5 V to -1.1 V, and the tested samples have good reproducibility more than three times (Figure 2b). In particular, the FE_{CO} of NiPc-DFP-Co COF can be as high as 99.86% at -0.9 V (vs. RHE), and the FE_{CO} could be maintained more than 99% among the potential range from -0.9 to -1.1 V (Figure 2b). In contrast, the potential for the highest FE_{CO} is negatively shifted by 0.2 V for both NiPc-DFP COF (99.19%, -1.1 V) and NiPc-DFP-Ni COF (97.81%, -1.1 V) (Figure 2b). As comparison, we have also prepared Co-salphen[40, 41] and it exhibits a highest FE_{CO} of 72.01% at -0.8 V, indicating the co-electrolysis ability of Co-salphen that can assist the electrocatalytic performance of NiPc (Figure S14 and S19). Besides, the j_{CO} of NiPc-DFP-Co COF is ~-12.43 mA cm^{-2} at -0.9 V, which is much higher with that of NiPc-DFP COF (-7.20 mA cm^{-2}) and NiPc-DFP-Ni COF (-9.10 mA cm^{-2}) (Figure 2d). In addition, the Tafel slope reflecting the dynamic activity of electrocatalytic CO_2RR shows that the Tafel slope of NiPc-DFP-Co COF is only 264.9 mV dec^{-1}, which is much smaller than that of NiPc-DFP COF (461.3 mV dec^{-1}) and NiPc-DFP-Ni COF (302.7 mV dec^{-1}) (Figure 2c). This indicates that the NiPc-DFP-Co COF has good kinetics in electrocatalytic CO_2RR, which may be attributed to the larger active surface and more efficient charge-transfer ability during the catalytic process.[42, 43] In addition, the transition frequency (TOF) of NiPc-DFP-Co COF is calculated to be 294 h^{-1} at -0.9 V, which is also larger than that of NiPc-DFP COF (154 h^{-1} at -0.9 V) and NiPc-DFP-Ni COF (195 h^{-1} at -0.9 V) (Figure 2d). In order to verify the charge transfer ability of them during the electrocatalytic CO_2RR process, electrochemical impedance spectroscopy (EIS) tests of NiPc-DFP COF, NiPc-DFP-Ni COF and NiPc-DFP-Co COF have been conducted (Figure S20). The results show that the charge transfer resistance of NiPc-DFP-Co COF is the smallest, indicating that the interfacial charge

This article presented here has been accepted for publication in CCS Chemistry and is posted at the request of the author prior to copyediting and composition.
© 2022 Chinese Chemical Society.

RESEARCH ARTICLE

transfer process is fastest when the Co^{2+} is incorporated into the salphen pockets.

Long-term stability is a key factor to evaluate the durability of the electrocatalysts in CO_2 electroreduction.[6] To evaluate the long-term stability, NiPc-DFP-Co COF is tested in 0.5 M $KHCO_3$ electrolyte filled with saturated CO_2 for 30 h (at -0.9 V) (Figure S21). The corresponding FE_{CO} can be remained stable current density during the long-term test, indicating that NiPc-DFP-Co COF is a kind of stable electrocatalyst. Furthermore, ^{13}C isotope labeling experiments have also been carried out and ^{13}CO (m/z = 29) is detected in the mass spectrometer, thus confirming that CO is produced from CO_2 electroreduction rather than catalyst decomposition (Figure S22).

Light-assisted electrocatalytic CO_2RR

Based on above mentioned results, the obtained NiPc-DFP-Co COF with the integrated nickel phthalocyanine and Co-salphen pocket units has exhibited excellent electrocatalytic CO_2RR performance. Notably, MPc, as a kind of light sensitive unit, is widely used photo-/electro-catalysis and might significantly improve the activity and energy efficiency under light irradiation.[19] As shown in the UV-Vis absorption spectra, NiPc-DFP COF and NiPc-DFP-M COF (M = Ni and Co) present visible light absorption ability (Figure S23). Moreover, the LSV curves under dark and light conditions of them have been studied and show significantly enhanced current density for all of them (Figure 3a, S24 and S25). According to the light-current response tests of NiPc-DFP-Co COF at different potentials, the current density is significantly improved under light irradiation (Figure 3e) and there is even a small light-current response detected under Ar atmosphere (Figure S26). Similarly, NiPc-DFP COF and NiPc-DFP-Ni COF also exhibit strong light-current response (Figure S27 and S28).

In addition, the light-assisted FE test results show that the FE_{CO} of the NiPc-DFP-Co COF can reach to ~100% at -0.7 V to -1.1 V, which is largely improved than dark conditions and represented to be one of the best performances in reported COFs (Figure 3b, Figure S29 and Table S2).[44, 45] Interestingly, a highest energy efficiency of ~69.78% can be achieved at -0.7 V (Figure S30), which is higer than that of NiPc-DFP-COF and NiPc-DFP-Ni COF (Figure S31 and S32). By contrast, the performance under dark condition can reach highest energy efficiency of ~62.82% at -0.9 V (Figure S30). In addition, the light-assisted electrocatalytic CO_2RR stability test shows that the FE_{CO} remains basically intact with slightly increased current density in 10 h (Figure S33). The NiPc-DFP-Co COF is confirmed to maintain its original structure and crystallinity by TEM and PXRD tests after electrolysis (Figure S34 and S35). Thus, NiPc-DFP-Co COF is an efficient and highly selective light-assisted electrocatalytic CO_2RR electrocatalyst.

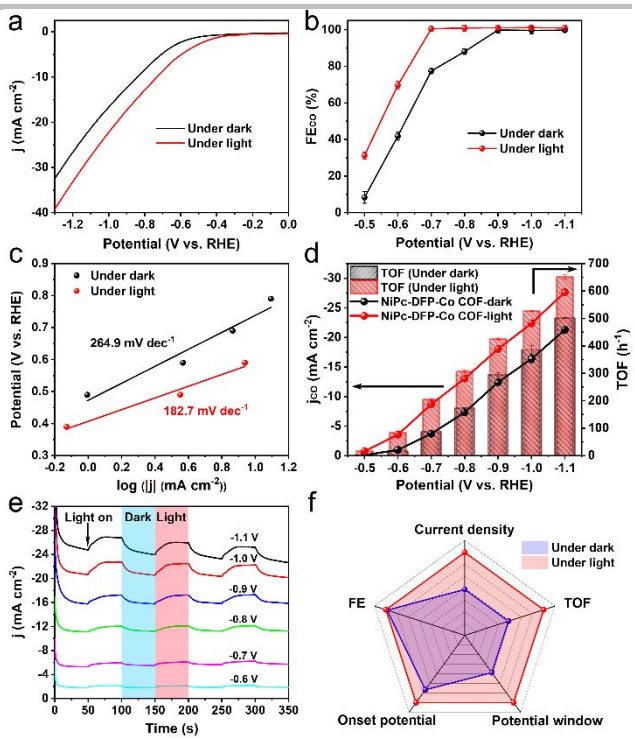

Figure 3 | *Evaluation of the electrocatalytic CO_2RR performance for NiPc-DFP-Co COF in light-assisted electrochemical measurements.* ***(a)*** *Comparison of LSV curves of NiPc-DFP-Co COF under dark and light conditions.* ***(b)*** *FE_{CO} of NiPc-DFP-Co COF under dark and light conditions.* ***(c)*** *Tafel plot of NiPc-DFP-Co COF under dark and light conditions.* ***(d)*** *j_{CO} and TOF at different potentials under dark and light conditions.* ***(e)*** *Light-current response curve of NiPc-DFP-Co COF at different bias voltages in H-cell.* ***(f)*** *The radar chart of performance comparison for NiPc-DFP-Co COF.*

The catalytic kinetics of the electrocatalysts under dark and light conditions are evaluated and relative values are calculated from the Tafel slopes. The calculation results show that the Tafel slope of NiPc-DFP-Co COF under light irradiation (182.7 mV dec^{-1}) is much smaller than that under dark condition (264.9 mV dec^{-1}) (Figure 3c), indicating that the light energy is beneficial to improve the kinetics of electrocatalytic CO_2RR.[14] Furthermore, the TOF and j_{CO} at different potentials of NiPc-DFP-Co COF are investigated under both dark and light conditions. The results show that both TOF and j_{CO} show an obvious enhancement under light irradiation in a wide potential range from -0.5 V to -1.1 V (Figure 3d). Based on the above experimental results, we made a radar chart of the performance for NiPc-DFP-Co COF. As shown in Figure 3f, NiPc-DFP-Co COF has broader potential window, lower onset potential, and higher TOF, current density and FE_{CO} under light irradiation condition when compared with that of under dark condition. Besides, NiPc-DFP COF and NiPc-DFP-Ni COF also present similarly enhanced performances under light irradiation, yet the-obtained performances for them are still inferior to NiPc-DFP-Co COF, suggesting the superiority of NiPc-DFP-Co COF under both dark and light irradiation conditions (Figure S24, S25 and S36). For example, FE_{CO} of NiPc-DFP-Co COF under light irradiation can reach to ~100% at -0.7 V (vs. RHE),

This article presented here has been accepted for publication in CCS Chemistry and is posted at the request of the author prior to copyediting and composition.
© 2022 Chinese Chemical Society.

RESEARCH ARTICLE

which is significantly higher than that of NiPc-DFP COF (86.28%, -0.7 V). Therefore, it can be concluded that the light irradiation can strongly enhance the electrocatalytic CO_2RR activity by interfering with the electron transfer properties of MPc COFs.

The DFT calculations and reaction mechanism

To investigate the electrocatalytic mechanisms, the detailed free energy profiles for each reaction coordinate during CO_2-to-CO pathways on these COFs have been calculated by using DFT calculations to confirm the active sites. In general, the formation of CO includes CO_2 adsorption/activation to generate $*CO_2$, then forms *COOH and further *CO, finally CO desorbs.[30] For NiPc-DFP COF with NiPc site, it has strong adsorption interaction with CO_2 yet relatively weak interaction with *COOH. Thus, the calculated energy barrier for $*CO_2$ is 0.68 eV and the formation of *COOH is the rate-determining step with a high energy barrier of 1.76 eV (Figure 4a and S37). We further set out to study the NiPc-DFP-Co COF and find that although Ni and Co metal sites simultaneously exist in NiPc-DFP-Co COF, the calculated binding energies of $*CO_2$ and *COOH on NiPc site and Co-salphen pocket (Co-N_2O_2) site are quite different. According to the calculated results, the Co-N_2O_2 site has a much stronger interaction with the *COOH intermediate than NiPc site and the *COOH formation step is a spontaneous process (Figure 4a, b and S38, S39). Besides, the rate-determining step of Co-N_2O_2 site is formation of $*CO_2$ (energy barrier, 0.82 eV). Interestingly, with the addition of Co-N_2O_2 site, the calculated binding energy of *COOH on NiPc site for the rate-determining step of NiPc site is largely decreased (1.39 eV) when compared with that of NiPc site (1.76 eV) in NiPc-DFP COF. For NiPc-DFP-Ni COF, the calculated binding energy profiles on Ni-salphen pocket (Ni-N_2O_2) site follows similar trend as that of NiPc site (Figure S40 and S41), which is quite different from that of Co-N_2O_2 in NiPc-DFP-Co COF. The addition of Ni-N_2O_2 site can slightly affect the energy barrier of NiPc site with the energy barrier (*COOH formation) value only decreases to 1.72 eV. This result is consistent with the obtained performance results of NiPc-DFP-Co COF when compared with NiPc-DFP COF and NiPc-DFP-Ni COF), in which the potential for the highest FE_{CO} is positively shifted by 0.2 V. In addition, in order to further understand the influence of Co-N_2O_2 site on the NiPc site, the electron cloud densities of NiPc-DFP COF and NiPc-DFP-Co COF have also calculated. The results show that the NiPc site loses 0.87 e in NiPc-DFP-Co COF, which is less than that in NiPc-DFP COF (0.93 e) (Figure 4c, d). This indicates that the intruducing of Co-N_2O_2 site can enhance the electron cloud density of NiPc site to construct the built-in electric field, and thus further complying with above calculated results in decreasing energy barrier of rate-determining step for the improvement of electrocatalytic CO_2RR activity.

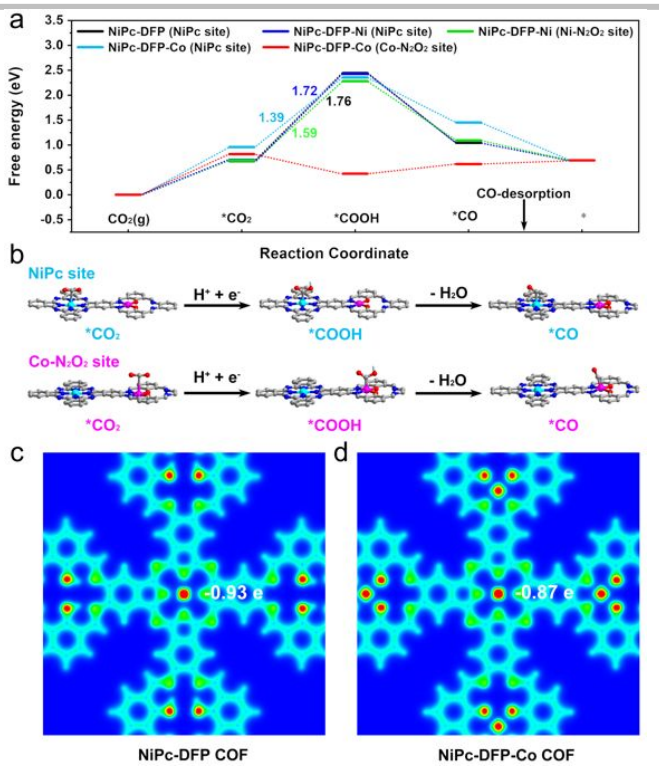

Figure 4 | *Mechanism and DFT calculations.* ***(a)*** *Free energy profiles for CO_2-to-CO reaction pathway on NiPc-DFP COF and NiPc-DFP-M COF (M = Ni and Co) at NiPc and M-N_2O_2 (M = Ni and Co), respectively.* ***(b)*** *The CO_2-to-CO conversion reactive pathway and inter-mediate architectures over NiPc and Co-salphen pocket (Co-N_2O_2) molecule of NiPc-DFP-Co COF.* ***(c)*** *The electron cloud density at NiPc site of NiPc-DFP COF.* ***(d)*** *The electron cloud density at NiPc site of NiPc-DFP-Co COF.*

Conclusions

In conclusion, a series of bimetallic NiPc-DFP-M COF (M = Ni and Co) electrocatalysts have been successfully prepared and applied in light-assisted CO_2 electroreduction. With the integrated modifiable salphen pockets, they possess advantages of outstanding light sensitivity, bimetallic catalytic centers in different coordination environments and built-in electric field effect. Best of them, NiPc-DFP-Co COF presents a superior FE_{CO} (~100%) in a wide potential range of -0.7 V to -1.1 V vs. RHE and a ~70% energy efficiency at -0.7 V under light irradiation, which is superior to those of mono-/homo-metallic COFs and under dark conditions and represented to be one of the best performances in reported COFs. The correlation between electrocatalytic CO_2RR selectivity and active sites have been intensively investigated via DFT calculations and electrocatalytic measurements. The high performance can be ascribed to the synergistic effect of NiPc and Co-salphen pockets that can largely reduce the rate-determining energy-barrier and enhance the electron-density to boost the light-assisted activity as supported by DFT-calculations. The design of such powerful bimetallic COF-based electrocatalysts not only proposes a synergistic catalytic strategy, but also provides intuitive understandings of product generation and catalyst optimization for photoelectric coupling electrocatalytic CO_2RR and beyond.

This article presented here has been accepted for publication in CCS Chemistry and is posted at the request of the author prior to copyediting and composition.
© 2022 Chinese Chemical Society.

Electrochemical measurements

The ECR activity measurements of the NiPc-DFP COF and NiPc-DFP-M COF (M = Co and Ni) catalysts were measured on the Biologic VSP electrochemical workstation at room temperature following our previous work.[19] Photo-assisted electrochemical measurements were performed in H-cell electrochemical system equipped with a 300 W Xe lamp (300-2500 nm, CEL-HXF300). The polarization curves results were obtained by performing linear sweep voltammetry (LSV) mode with a scan rate of 5 mV s^{-1} during the CO_2 reduction experiments. Electrochemical impedance spectroscopy (EIS) measurement was performed on the electrochemical analyzer in a frequency range from 100 kHz to 100 mHz by applying an AC voltage with 10 mV amplitude at -0.90 V *vs*. RHE. The applied carbon paper (thickness, ~0.19 mm) was purchased and used without further treatment.

Calculation methods

All the density functional theory (DFT) calculations were performed using the Vienna Ab initio Simulation Package (VASP) within the generalized gradient approximation (GGA) using the Revised Perdew-Burke-Ernzerhof (r-PBE) functional. Half atoms at bottom are fixed in all the calculations. The computational hydrogen electrode (CHE) model that proposed by Nørskov et al.[46] was applied to describe the free energy changes (ΔG) of reaction for CO_2RR elementary steps involving ($H^+ + e^-$) pair transfer.

Supporting Information

Supporting Information is available and includes 41 figures and 2 tables.

Declaration of Conflicts of interest

There are no conflicts to declare.

Acknowledgements

This study was financially supported by NSFC (Grants 21871141, 21871142, 22071109, 21901122, 22225109 and 22171139).

Author contributions

Y.-Q. L. and X. T. conceived the idea. X. T. designed the experiments, collected and analyzed the data. X. H., J.-W. S., R. W., J. Z., C. G., Y.-R. W., M. L. Q. L., Y. C. and S.-L. L. assisted with the experiments and characterizations. X. T. wrote the manuscript. All authors have approved the final version of the manuscript.

X. T., X. H. *and* J.-W. S. contributed equally to this work.

References

1. Anagnostou, E.; John, E. H.; Edgar, K. M.; Foster, G. L.; Ridgwell, A.; Inglis, G. N.; Pancost, R. D.; Lunt, D. J.; Pearson, P. N. Changing atmospheric CO_2 concentration was the primary driver of early Cenozoic climate. *Nature.* **2016**, *533*, 380-384.
2. Shukla, J. B.; Verma, M.; Misra A. K. Effect of global warming on sea level rise: A modeling study. *Ecol. Complex.* **2017**, 32, 99-110.
3. Nakata, K.; Ozaki, T.; Terashima, C.; Fujishima, A.; Einaga, Y. High-Yield Electrochemical Production of Formaldehyde from CO_2 and Seawater. *Angew. Chem. Int. Ed.* **2013**, *53*, 871.
4. Chu, S.; Cui, Y.; Liu, N. The path towards sustainable energy. *Nat. Mater.* **2017**, *16*, 16-22.
5. Ding, M.; Flaig, R. W.; Jiang, H.-L.; Yaghi, O. M. Carbon capture and conversion using metal-organic frameworks and MOF-based materials. *Chem. Soc. Rev.* **2019**, *48*, 2783.
6. Zhou, J. H.; Yuan, K.; Zhou, L.; Guo, Y.; Luo, M. Y.; Guo, X. Y.; Meng, Q. Y.; Zhang, Y. W. Boosting Electrochemical Reduction of CO_2 at a Low Overpotential by Amorphous Ag-Bi-S-O Decorated Bi Nanocrystals. *Angew. Chem. Int. Ed.* **2019**, *131*, 14335.
7. Liu, J.; Yang, D.; Zhou, Y.; Zhang, G.; Xing, G.; Liu, Y.; Ma, Y.; Terasaki, O.; Yang, S.; Chen, L. Tricycloquinazoline-Based 2D Conductive Metal-Organic Frameworks as Promising Electrocatalysts for CO_2 Reduction. *Angew. Chem. Int. Ed.* **2021**, *60*, 14473-14479.
8. Francke, R.; Schille, B.; Roemelt, M. Homogeneously Catalyzed Electroreduction of Carbon Dioxide-Methods, Mechanisms, and Catalysts. *Chem. Rev.* **2018**, *118*, 4631.
9. Yi, J. D.; Xie, R.; Xie, Z. L.; Chai, G. L.; Liu, T. F.; Chen, R. P.; Huang, Y. B.; Cao, R. Highly Selective CO_2 Electroreduction to CH_4 by In Situ Generated Cu_2O Single-Type Sites on a Conductive MOF: Stabilizing Key Intermediates with Hydrogen Bonding. *Angew. Chem. Int. Ed.* **2020**, *59*, 23641-23648.
10. Wang, Y. R.; Ding, H. M.; Ma, X. Y.; Liu, M.; Yang, Y. L.; Chen, Y.; Li, S. L.; Lan, Y. Q. Imparting CO_2 Electroreduction Auxiliary for Integrated Morphology Tuning and Performance Boosting in a Porphyrin-based Covalent Organic Framework. *Angew. Chem. Int. Ed.* **2022**, *61*, e202114648.
11. Wang, Y. R.; Yang, R. X.; Chen, Y.; Gao, G. K.; Wang, Y. J.; Li, S. L.; Lan, Y. Q. Chloroplast-like porous bismuth-based core-shell structure for high energy efficiency CO_2 electroreduction. *Sci. Bull.* **2020**, *65*, 1635.
12. Diercks, C. S.; Lin, S.; Kornienko, N.; Kapustin, E. A.; Nichols, E. M.; Zhu, C.; Zhao, Y.; Chang, C. J.; Yaghi, O. M. Reticular Electronic Tuning of Porphyrin Active Sites in Covalent Organic Frameworks for Electrocatalytic Carbon Dioxide Reduction. *J. Am. Chem. Soc.* **2018**, *140*, 1116-1122.
13. Liu, H.; Chu, J.; Yin, Z.; Cai, X.; Zhuang, L.; Deng, H. Covalent Organic Frameworks Linked by Amine Bonding for Concerted Electrochemical Reduction of CO_2. *Chem.* **2018**, *4*, 1696-1709.
14. Yang, D.; Yu, H.; He, T.; Zuo, S.; Liu, X.; Yang, H.; Ni, B.; Li, H.; Gu, L.; Wang, D. Visible-light-switched electron transfer over single porphyrin-metal atom center for highly selective electroreduction of carbon dioxide. *Nat. Commun.* **2019**, *10*, 3844.
15. Wu, Q.; Xie, R.-K.; Mao, M.-J.; Chai, G.-L.; Yi, J.-D.; Zhao, S.-S.; Huang, Y.-B.; Cao, R. Integration Strong Electron Transporter Tetrathiafulvalene into Metalloporphyrin-based Covalent Organic Framework

This article presented here has been accepted for publication in CCS Chemistry and is posted at the request of the author prior to copyediting and composition.
© 2022 Chinese Chemical Society.

for Highly Efficient Electroreduction of CO_2. *ACS Energy Lett.* **2020**, *5*, 1005-1012.
16. Lu, M.; Liu, J.; Li, Q.; Zhang, M.; Liu, M.; Wang, J. L.; Yuan, D. Q.; Lan, Y. Q. Rational Design of Crystalline Covalent Organic Frameworks for Efficient CO_2 Photoreduction with H_2O. *Angew. Chem. Int. Ed. Engl.* **2019**, *58*, 12392-12397.
17. Cheung, P. L.; Lee, S. K.; Kubiak, C. P. Facile Solvent-Free Synthesis of Thin Iron Porphyrin COFs on Carbon Cloth Electrodes for CO_2 Reduction. *Chem. Mater.* **2019**, *31*, 1908.
18. Zhang, Y.; Zhong, R.-L.; Lu, M.; Wang, J.-H.; Jiang, C.; Gao, G.-K.; Dong, L.-Z.; Chen, Y.; Li, S. L.; Lan, Y. Q. Single Metal Site and Versatile Transfer Channel Merged into Covalent Organic Frameworks Facilitate High-Performance Li-CO_2 Batteries. *ACS Cent. Sci.* **2021**, *7*, 175-182.
19. Lu, M.; Zhang, M.; Liu, C. G.; Liu, J.; Shang, L. J.; Wang, M.; Chang, J. N.; Li, S. L.; Lan, Y. Q. Stable Dioxin-Linked Metallophthalocyanine Covalent Organic Frameworks (COFs) as Photo-Coupled Electrocatalysts for CO_2 Reduction. *Angew. Chem. Int. Ed.* **2021**, *60*, 4864-4871.
20. Nikoloudakis, E.; López-Duarte, I.; Charalambidis, G.; Ladomenou, K.; Ince, M.; Coutsolelos, A. G. Porphyrins and phthalocyanines as biomimetic tools for photocatalytic H_2 production and CO_2 reduction. *Chem. Soc. Rev.* **2022**, DOI: 10.1039/d2cs00183g.
21. Gao, Y.; Zhang, R.; Xiang, Z.; Yuan, B.; Cui, T.; Gao, Y.; Cheng, Z.; Wu, J.; Qi, Y.; Zhang, Z. Theoretical insights into photocatalytic CO_2 reduction on Palladium phthalocyanine. *Chem. Phys. Lett.* **2022**, *803*, 139812.
22. Kaya, E. Ç.; Ersoy, S.; Durmuş, M.; Kantekin, H. Synthesis of fluorine-containing phthalocyanines and investigation of the photophysical and photochemical properties of the metal-free and zinc phthalocyanines. *Heterocycl. Commun.* **2018**, *24*, 259-265.
23. Huang, N.; Lee, K. H.; Yue, Y.; Xu, X.; Irle, S.; Jiang, Q.; Jiang, D. A Stable and Conductive Metallophthalocyanine Framework for Electrocatalytic Carbon Dioxide Reduction in Water. *Angew. Chem. Int. Ed.* **2020**, *59*, 16587-16593.
24. Liang, Z.; Wang, H. Y.; Zheng, H.; Zhang, W.; Cao, R. Porphyrin-based frameworks for oxygen electrocatalysis and catalytic reduction of carbon dioxide. *Chem. Soc. Rev.* **2021**, *50*, 2540-2581.
25. Dong, X. Y.; Si, Y. N.; Wang, Q. Y.; Wang, S.; Zang, S.Q. Integrating single atoms with different microenvironments into one porous organic polymer for efficient photocatalytic CO_2 reduction. *Adv. Mater.* **2021**, *33*, 2101568.
26. Lu, M.; Zhang, M.; Liu, J.; Chen, Y.; Liao, J. P.; Yang, M. Y.; Cai, Y. P.; Li, S. L.; Lan, Y. Q. Covalent Organic Framework Based Functional Materials: Important Catalysts for Efficient CO_2 Utilization. *Angew. Chem. Int. Ed.* **2022**, *61*, e202200003.
27. Zhang, M. D.; Si, D. H.; Yi, J. D.; Zhao, S. S.; Huang, Y. B.; Cao, R. Conductive Phthalocyanine-Based Covalent Organic Framework for Highly Efficient Electroreduction of Carbon Dioxide. *Small.* **2020**, *16*, e2005254.
28. Yue, Y.; Cai, P.; Xu, K.; Li, H.; Chen, H.; Zhou, H.-C.; Huang, N. Stable Bimetallic Polyphthalocyanine Covalent Organic Frameworks as Superior Electrocatalysts. *J. Am. Chem. Soc.* **2021,** *143*, 18052-18060.
29. Lin, S.; Diercks, C. S.; Zhang, Y.-B.; Kornienko, N.; Nichols, E. M.; Zhao, Y.; Paris, A. R.; Kim, D.; Yang, P.; Yaghi, O. M. Covalent organic frameworks comprising cobalt porphyrins for catalytic CO_2 reduction in water. *Science.* **2015**, *349*, 1208.
30. Zhu, H. L.;Chen, H. Y.; Han, Y. X.; Zhao, Z. H.; Liao, P. Q.; Chen, X. M. A Porous π-π Stacking Framework with Dicopper(I) Sites and Adjacent Proton Relays for Electroreduction of CO_2 to C_{2+} Products. *J. Am. Chem. Soc.* **2022**, *144*, 13319.
31. Yuan, J.; Chen, S.; Zhang, Y.; Li, R.; Zhang, J.; Peng, T. Structural Regulation of Coupled Phthalocyanine-Porphyrin Covalent Organic Frameworks to Highly Active and Selective Electrocatalytic CO_2 Reduction. *Adv. Mater.* **2022**, *34*, e2203139.
32. Yi, H. T.; Rangan, S.; Tang, B.; Frisbie, C. D.; Podzorov, V. Electric-field effect on photoluminescence of lead-halide perovskites. *Mater. Today.* **2019**, *28*, 31-39.
33. Tian, Y. S.; Chen, Z. B. Electronic Structures and Spectra Properties of Plasma-Embedded Atoms or Ions Under the External Electric-Field. *Few-Body Syst.* **2022**, *63*, 19.
34. Habibi, M. H.; Mokhtari, R.; Mikhak, M.; Amirnasr, M.; Amiri, A. Synthesis, spectral and electrochemical studies of Cu(II) and Ni(II) complexes with new N_2O_2 ligands: a new precursor capable of depositing copper nanoparticles using thermal reduction. *Spectrochim. Acta A Mol. Biomol. Spectrosc.* **2011**, *79*, 1524.
35. Han, B.; Jin, Y.; Chen, B.; Zhou, W.; Yu, B.; Wei, C.; Wang, H.; Wang, K.; Chen, Y.; Chen, B.; Jiang, J. Maximizing Electroactive Sites in a Three-Dimensional Covalent Organic Framework for Significantly Improved Carbon Dioxide Reduction Electrocatalysis. *Angew. Chem. Int. Ed.* **2022**, *61*, e202114244.
36. Yuan, L.**;** Zhang, L.; Li, X.-X.; Liu, J.; Liu, J.-J.; Dong, L.-Z.; Li, D.-S.; Li, S. L.; Lan, Y. Q. Uncovering the synergistic photocatalytic behavior of bimetallic molecular catalysts. *Chin. Chem. Lett.* **2022**, DOI: 10.1016/j.cclet.2022.01.039.
37. Gao, D.; Liu, T.; Wang, G.; Bao, X. Structure Sensitivity in Single-Atom Catalysis toward CO_2 Electroreduction. *ACS Energy Lett.* **2021**, *6*, 713-727.
38. Li, T.**;** Zhang, W.-D.; Liu, Y.; Li, Y.; Cheng, C.; Zhu, H.; Yan, X.; Li, Z.; Gu, Z.-G. A two-dimensional semiconducting covalent organic framework with nickel(II) coordination for high capacitive performance. *J. Mater. Chem. A***.** **2019**, *7*, 19676.
39. Deng, F.; Li, X.; Ding, F.; Niu, B.; Li, J. Pseudocapacitive Energy Storage in Schiff Base Polymer with Salphen-Type Ligands. *J. Phys. Chem. C.* **2018**, *122*, 5325.
40. Xue, D.; Lv, Q. Y.; Lin, C. N.; Zhan, S. Z. Function of 7, 7, 8, 8-tetracyanoquinodimethane (TCNQ) on electrocatalytic hydrogen generation catalyzed by N, N '-benzene bis (salicylideniminato)nickel (II). *Polyhedron.* **2016**, *117*, 300.

This article presented here has been accepted for publication in CCS Chemistry and is posted at the request of the author prior to copyediting and composition.
© 2022 Chinese Chemical Society.

41. Wang, Y. R.; Huang, Q.; He, C. T.; Chen, Y.; Liu, J.; Shen, F. C.; Lan, Y. Q. Oriented electron transmission in polyoxometalate-metalloporphyrin organic framework for highly selective electroreduction of CO. *Nat. Commun.* **2018**, *9*, 4466.
42. Zhu, H. J.; Lu, M.; Wang, Y. R.; Yao, S. J.; Zhang, M.; Kan, Y. H.; Liu, J.; Chen, Y.; Li, S. L.; Lan, Y. Q. Efficient electron transmission in covalent organic framework nanosheets for highly active electrocatalytic carbon dioxide reduction. *Nat. Commun.* **2020**, *11*, 497.
43. Wu, Q.; Mao, M. J.; Wu, Q. J.; Liang, J.; Huang, Y. B.; Cao, R. Construction of Donor-Acceptor Heterojunctions in Covalent Organic Framework for Enhanced CO_2 Electroreduction. *Small*. **2021**, *17*, e2004933.
44. He, Z.; Goulas, J.; Parker, E.; Sun, Y.; Zhou, X. D.; Fei, L. Review on covalent organic frameworks and derivatives for electrochemical and photocatalytic CO_2 reduction. *Catal. Today.* **2022**, DOI: 10.1016/j.cattod.2022.04.021.
45. An, S.; Lu, C.; Xu, Q.; Lian, C.; Peng, C.; Hu, J.; Zhuang, X.; Liu, H. Constructing Catalytic Crown Ether-Based Covalent Organic Frameworks for Electroreduction of CO_2. *ACS Energy Lett.* **2021**, *6*, 3496-3502.
46. Peterson, A. A.; Abild-Pedersen, F.; Studt, F.; Rossmeisl, J.; Nørskov, J. K. How copper catalyzes the electroreduction of carbon dioxide into hydrocarbon fuels. Energy Environ. Sci. **2010**, 3, 1311-1315.

This article presented here has been accepted for publication in CCS Chemistry and is posted at the request of the author prior to copyediting and composition.
© 2022 Chinese Chemical Society.

RESEARCH ARTICLE

Entry for the Table of Contents

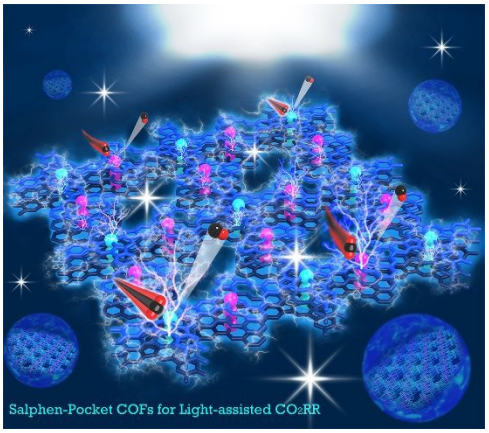

A series of bimetallic Pc-based NiPc-DFP-M COF (M = Ni and Co) with integrated salphen-pockets and NiPc units have been synthesized and successfully applied in efficient light-assisted CO_2 electroreduction.

This article presented here has been accepted for publication in CCS Chemistry and is posted at the request of the author prior to copyediting and composition.
© 2022 Chinese Chemical Society.